VCP–adaptor interactions are exceptionally dynamic and subject to differential modulation by a VCP inhibitor

Liang Xue[1], Emily E. Blythe[1], Elyse C. Freiberger[2], Jennifer Mamrosh[1], Alexander S. Hebert[3], Justin M. Reitsma[1], Sonja Hess[5], Joshua J. Coon[2,3,4], and Raymond Deshaies[1,6,7]

SUPPLEMENTAL FIGURE LEGENDS

Supplemental Fig. S1: Analysis of VCP complexes by SEC-mass spectrometry. ***A***, Time course of efficiency of VCP knockdown induced by doxycycline (1µg/ml) using HEK293 cell line that has a stably integrated, doxycycline-inducible VCP shRNA (DTC204). At the indicated time after transfection, cell lysate was prepared and evaluated by SDS-PAGE and Western blotting with anti-VCP. The 5 day point was chosen as the condition for all MS experiments, since on day 6 a large amount of cell death occurred. ***B***, Violin plots showing the distribution of coefficients of variation (n=3) of apex measurements for proteins in each sample. ***C***, Number of proteins quantified in each experiment (mean ± SEM, n=3). ***D***, Total abundance change (defined as $[\text{LFQintensity}]_{\text{treated}}$ divided by $[\text{LFQintensity}]_{\text{control}}$) for all detected proteins in response to VCP knockdown (left panel) or NMS873 treatment (right panel). ***E***, DAVID gene ontology keywords for proteins whose mean apex position was increased or decreased by > 2.5 fractions upon NMS873 treatment or VCP knockdown. ***F***, Proteins from **Fig. 1B** with a shift in mean apex position of >2.5 fractions, along with a >4 fold increase or decrease in abundance following VCP knockdown. PTPN9 (marked with **) is the only protein that met these criteria in both the VCP knockdown and NMS873 (panel G) treatment groups. Proteins in red have been reported either in BioGRID or in the published literature to bind and/or interact with VCP in some manner. ***G***,

Same as panel E, except for the experiment in **Fig. 1C** in which cells were treated with 10 μM NM873 for 6h.

Supplemental Fig. S2: Fractionation of VCP adaptors by SEC. SEC fractionation behavior of different classes of VCP adaptors upon perturbation of VCP activity by NMS873 or shRNA-mediated depletion. ***A***, Class I adaptors co-fractionated with VCP. ***B***, Class II adaptors were constitutively assembled in complexes of higher MW than the VCP peak. ***C***, Class III adaptors fractionated at MWs lower than VCP and were not affected by either chemical inhibition or depletion of VCP. ***D***, The relative LFQ intensities of VCP and adaptors in SEC fractions from HEK293 cells (bars represent standard error of the mean, n=3). ***E***, HEK293 lysate from untreated cells was chromatographed on a Superose 6 column, and 1 mL fractions were analyzed via western blot. ***F***, *In silico*-generated SEC chromatograms of representative VCP adaptors in the Kirkwood et. al. dataset.

Supplemental Fig. S3: Control experiments for VCP immunoprecipitation. ***A***, Western blotting shows the expression of endogenous VCP bearing an N-terminal FLAG tag in HEK293 cells. Lysates of $HEK293^{FLAGVCP}$ cells were incubated with anti-VCP or anti-FLAG antibody. The input, flow through (FT) and bound fractions were separated by SDS-PAGE and blotted with anti-VCP or anti-FLAG antibody. Note that the FLAG tag did not cause a perceptible shift in the mobility of VCP. WB, Western blot. ***B***, VCP was recovered in IPs as short as 6 min. The time indicated above each lane is the duration of the incubation with antibody prior to adding protein A/G beads for an additional 5 min to capture immune complexes. As the IP time increased, the amount of VCP detected by Western blot decreased in the flow through and

increased in the elution. ***C***, Label-free quantification of VCP recovery in IPs of varying duration for the experiments in **Fig. 3A** and **Fig. 3B**. ***D***, Venn diagram shows the overlap in protein identifications comparing FLAG IP from HEK293^{FLAGVCP} cells with IP of untagged endogenous VCP from wild type HEK293 cells. n=1 ***E***, Enrichment of VCP adaptors in VCP pull-downs. Two experiments were conducted in parallel. In the first experiment (black bars), HEK293^{FLAGVCP} and HEK293 cells were grown in medium containing 'heavy' or 'light' lysine plus arginine, respectively. Cell lysates from both cultures were individually subjected to IP with anti-FLAG and following the IP step the samples were mixed and analyzed by mass spectrometry. In the second experiment (gray bars), Lysate from the 'heavy' HEK293 cells was subjected to IP with anti-VCP whereas lysate from the 'light' HEK293 cells was subjected to mock IP (no antibody was present before protein A/G beads added for capture). Following the IP step the samples were mixed and analyzed by mass spectrometry. The H/L ratios for known VCP-interacting proteins are shown. n=1.

Supplemental Fig. S4: Effect of ND1L 'sponge' on recovery of VCP binding proteins during immunoprecipitation. Titration of increasing amounts of 'light' ND1L into 'heavy' cell lysate progressively reduced the number of proteins recovered by IP with a VCP antibody that does not bind ND1L.

Supplemental Fig. S5: Crosslinked VCP complex can be purified by immunoprecipitation. When immunoprecipitated with anti-VCP for 2 hours, most of the cross-linked VCP was recovered in the bound fraction. VCP cross-links were largely resolved upon treating the bound fraction with the reducing agent DTT.

Supplemental Fig. S6: Chemical inhibition of VCP modulates its repertoire of associated adaptor proteins in HEK293 cells and BJ fibroblasts. ***A***, Label swap SILAC experiments were performed in which cells were either mock-treated or supplemented with 10 µM NMS873 for 6 hours. Cells were treated with 800 µM DSP for 30 minutes prior to cell lysis, mixing of cell lysates, IP with anti-VCP, and mass spectrometry analysis. The ratios for each protein identified in the replicate experiments are plotted on the x and y axes. ***B***, same as panel A, except that cells were treated with or without 10 µM MG132 for 2 hours. ***C***, Duplicate mass spectrometry experiments with label-free quantification were performed in which cells were either mock-treated or supplemented with 10 µM NMS873 for 6 hours. Cells were treated with 800 µM DSP for 30 minutes prior to cell lysis, mixing of cell lysates, IP with anti-VCP, and mass spectrometry analysis. The ratios for each protein identified in the replicate experiments are plotted on the x and y axes. ***D***, same as panel C, except that cells were treated with or without 10 µM MG132 for 2 hours.

Supplemental Fig. S7: Potential substrates for UFD1L–NPLOC4 and UBX domain proteins as determined by covariance analyses.

A

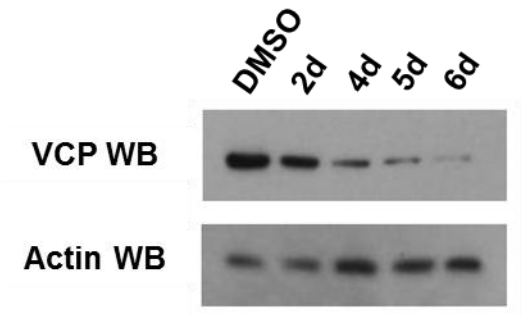

B

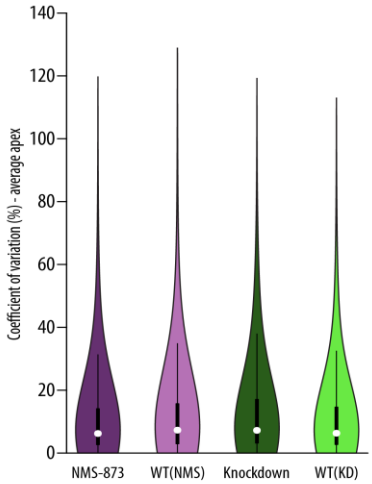

C

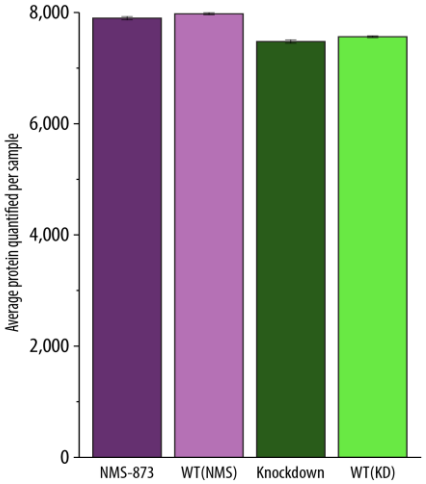

D

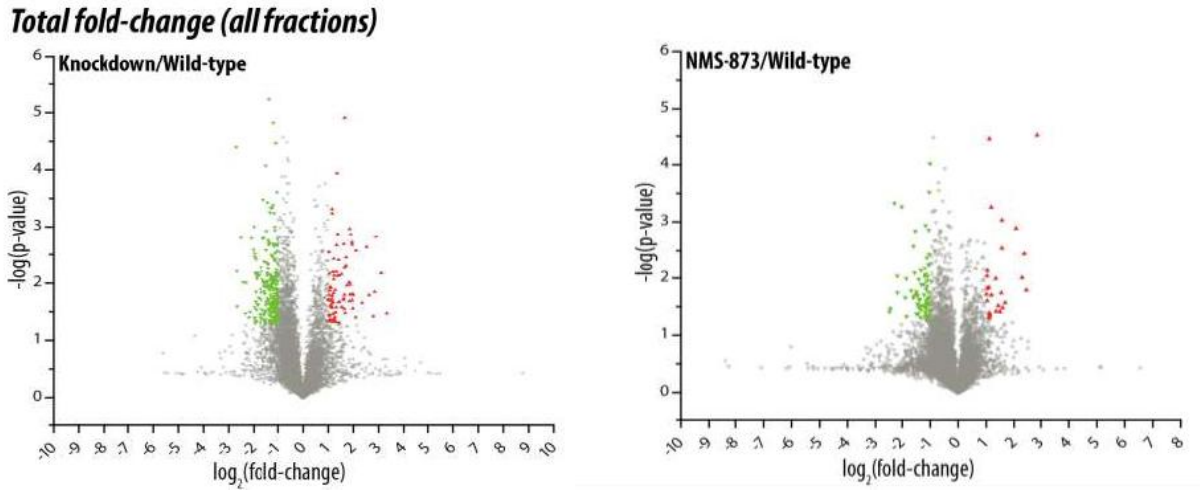

Supplemental Fig. 1

E

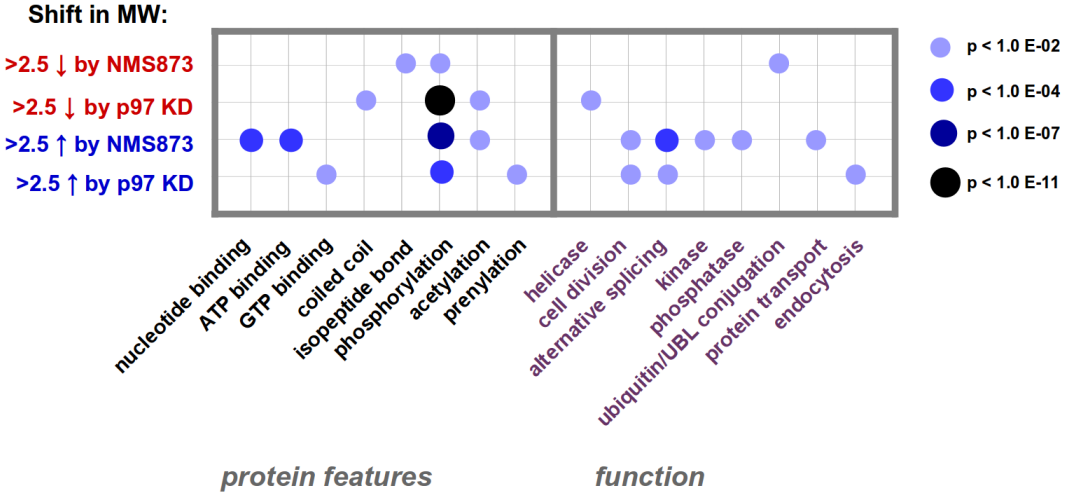

F

>2.5 increase in MW	>2.5 increase in MW	>2.5 decrease in MW	>2.5 decrease in MW
>4 fold increase in abundance	>4 fold decrease in abundance	>4 fold increase in abundance	>4 fold decrease in abundance
APLP2	ANAPC4	CALML5	ANK3
LDLR	ANKRD13A	DNAJB4	**ARFGEF2**
RAB33B	BBS7	DSG1	CAMKK1
SHQ1	BCL11A	ELOVL5	EIF3D
YDJC	BECN1	EPB41L5	TBK1
	CDC16	GALNT7	
	CDC42	GNG5	
	COG8	HIST1H1D	
	CSNK1A1	HMGN4	
	DECR2	KCTD10	
	EDEM3	RNH1	
	FAM160B1	SDAD1	
	FAM3C	SPAG5	
	GRB10	STK11IP	
	ITSN2	WDR91	
	KIAA0391		
	MED31		
	MFN2		
	NGRN		
	NKIRAS2		
	**PTPN9		
	RABGEF1		
	RMND5A		
	SATB2		
	SELH		
	SH3BP1		
	SLC30A9		
	TCP11L1		
	TEX264		
	TTC28		
	TUBAL3		

G

>2.5 increase in MW	>2.5 increase in MW	>2.5 decrease in MW	>2.5 decrease in MW
>4 fold increase in abundance	>4 fold decrease in abundance	>4 fold increase in abundance	>4 fold decrease in abundance
AZGP1	AP5S1	ELP5	**CDT1**
CTDSPL2	ARHGAP8	HPSE	DSC1
DACH2	ARHGEF6	ITGA1	MMAA
IRF6	BCKDHB	**S100A9**	RSRC1
RBKS	BCL2L1	SGOL1	TUBA1B
RTEL1	BCL2L12	SLC9A6	
S100A7	BCL7B	**SON**	
TIMP2	C10orf76	TTLL4	
	C11orf83	ZNF771	
	C5orf51		
	C7orf55		
	CBWD2		
	CCDC28B		
	CISD3		
	CRYGD		
	CYB5R4		
	DDX59		
	DSCC1		
	DYNC2LI1		
	ERAP1		
	ERI1		
	GLI3		
	IFIT5		
	INPP4A		
	ITPK1		
	KDM1B		
	KPTN		
	LENG9		
	LIN9		
	LRRC42		
	LZTS2		
	MALSU1		
	MAP2K7		
	MID1IP1		
	MOB3B		
	MTO1		
	NEK3		
	OSBPL2		
	PAIP2B		
	PGM5		
	POLR1C		
	PTPN14		
	**PTPN9		
	RAB34		
	RARS2		
	RCHY1		
	RPS6KB2		
	SCAI		
	SDCBP		
	SFR1		
	SGK3		
	SKA1		
	SNX21		
	STK39		
	TFE3		
	TRADD		
	TRMT13		
	UBE2E1		
	XRCC3		
	ZFPM1		

Supplemental Fig. 1

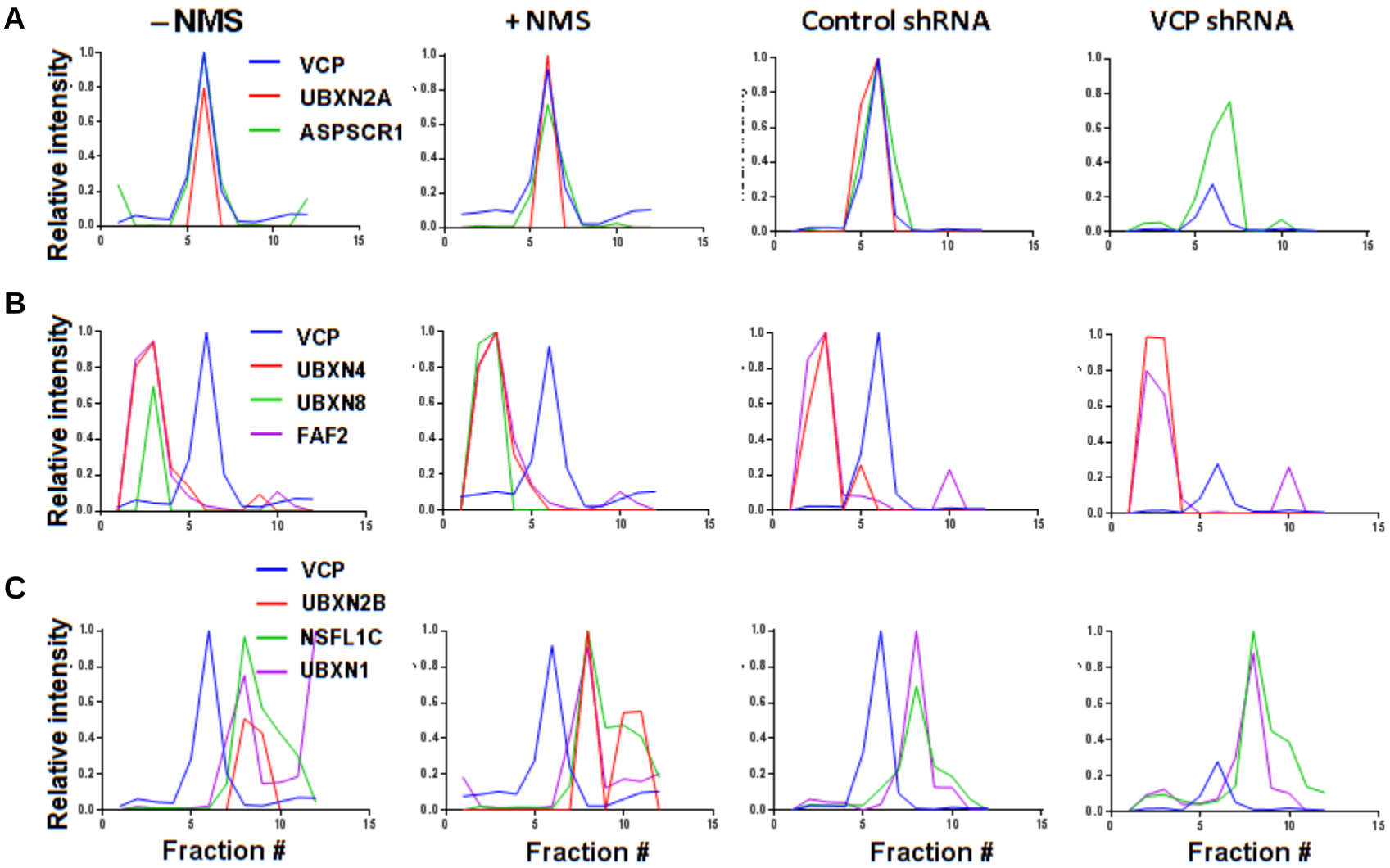

Supplemental Fig. 2

D

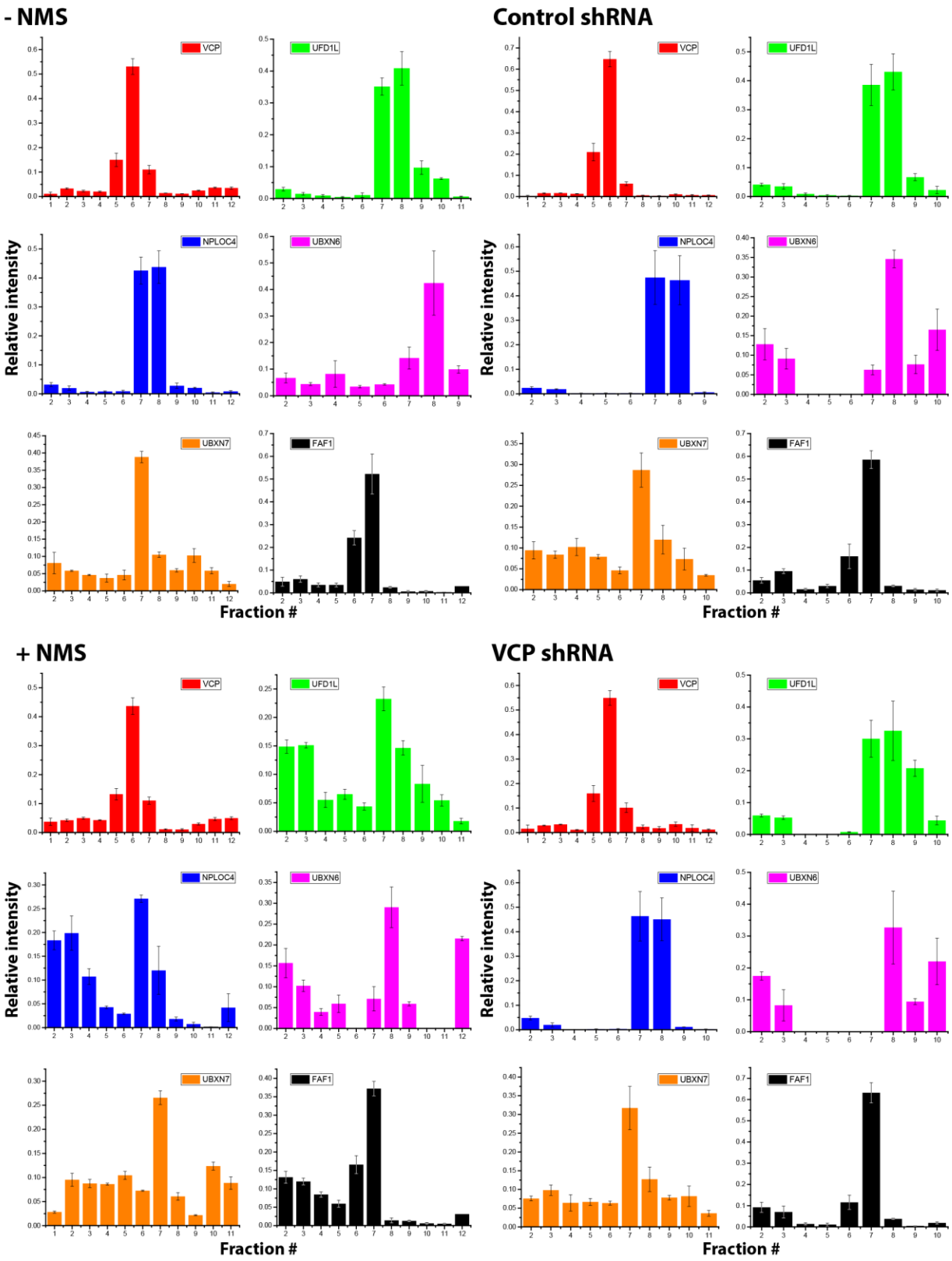

Supplemental Fig. 2

E

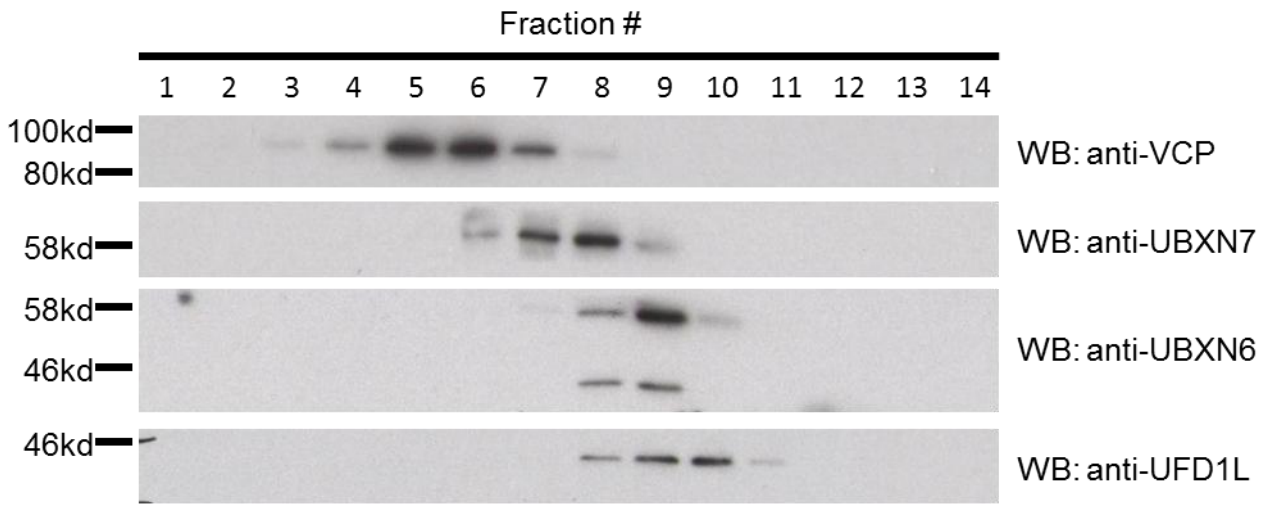

Supplemental Fig. 2

F

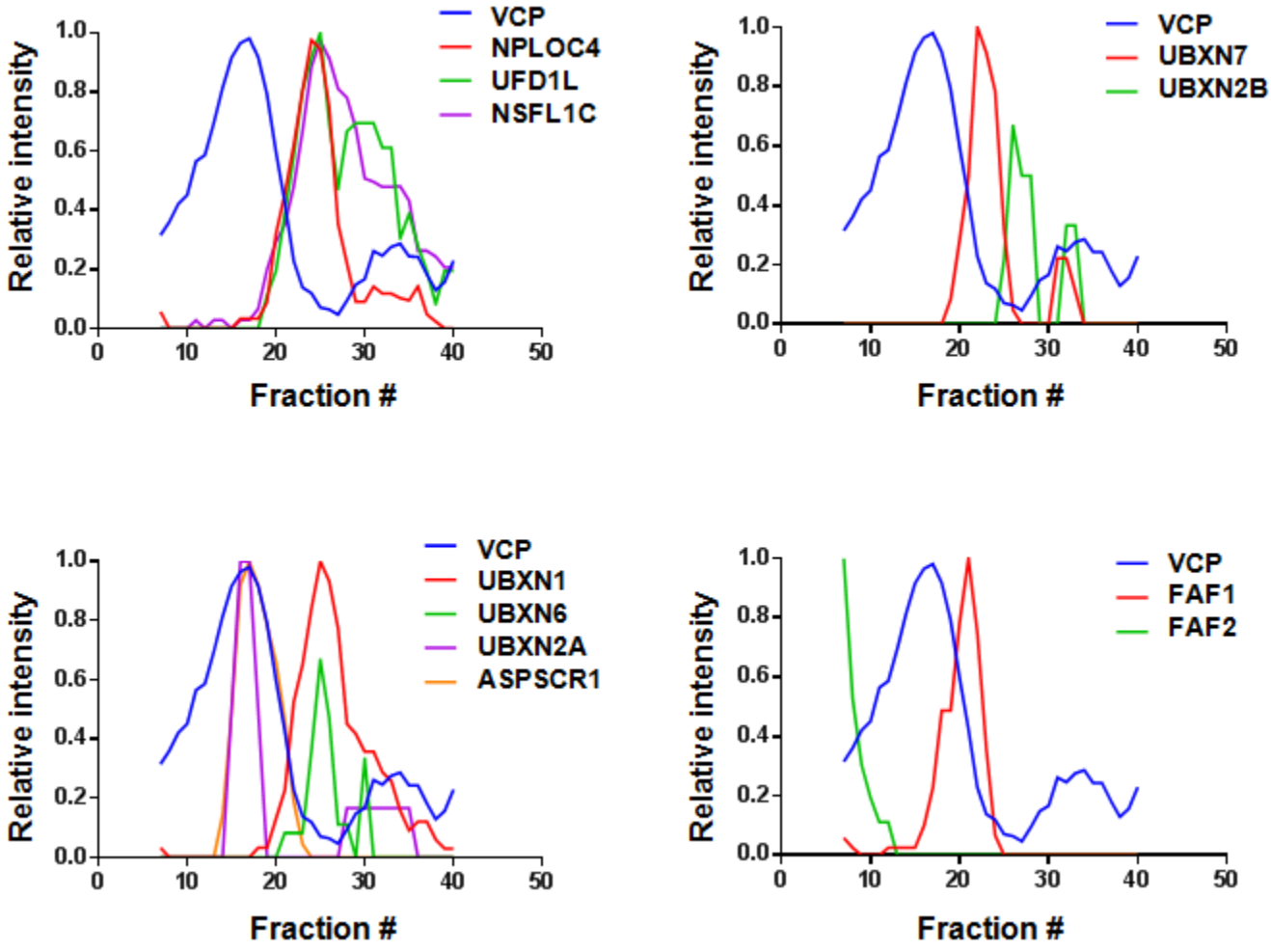

Supplemental Fig. 2

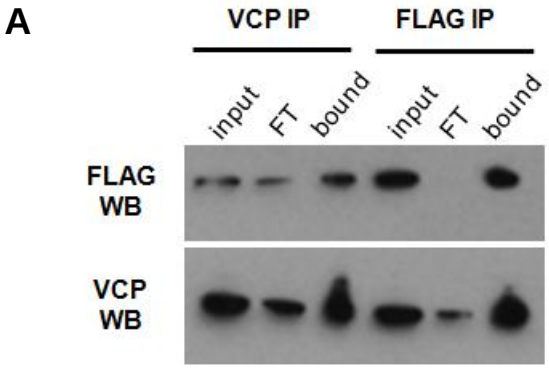

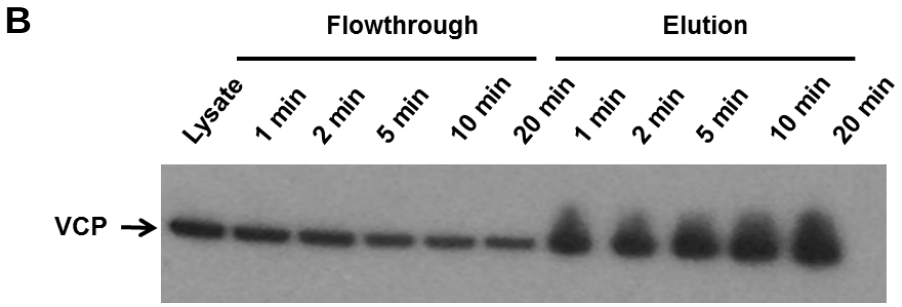

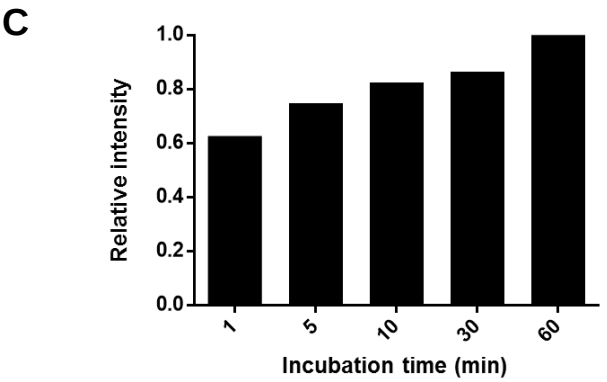

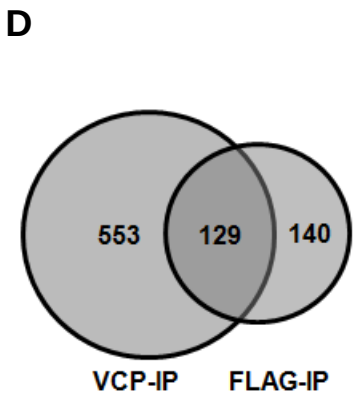

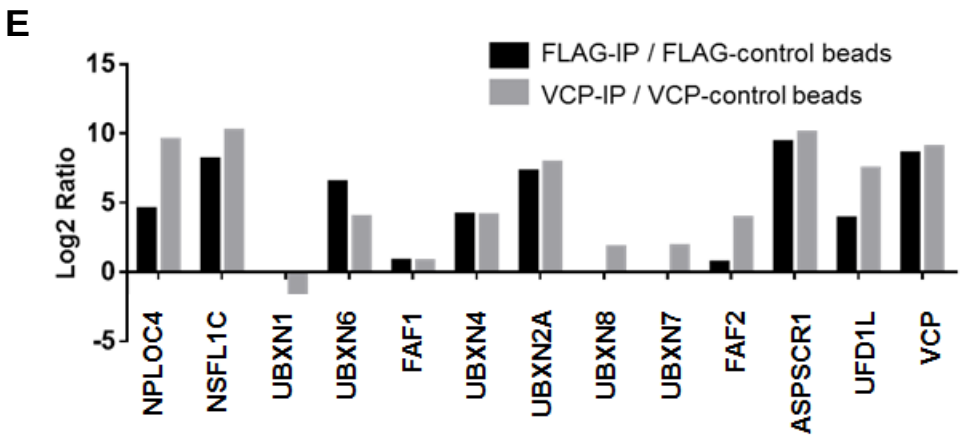

Supplemental Fig. 3

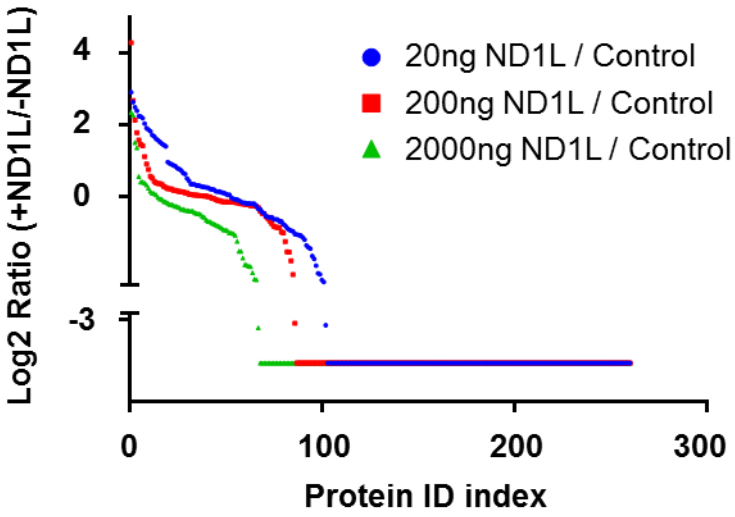

Supplemental Fig. 4

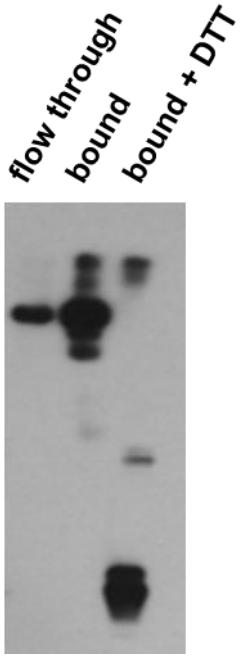

Supplemental Fig. 5

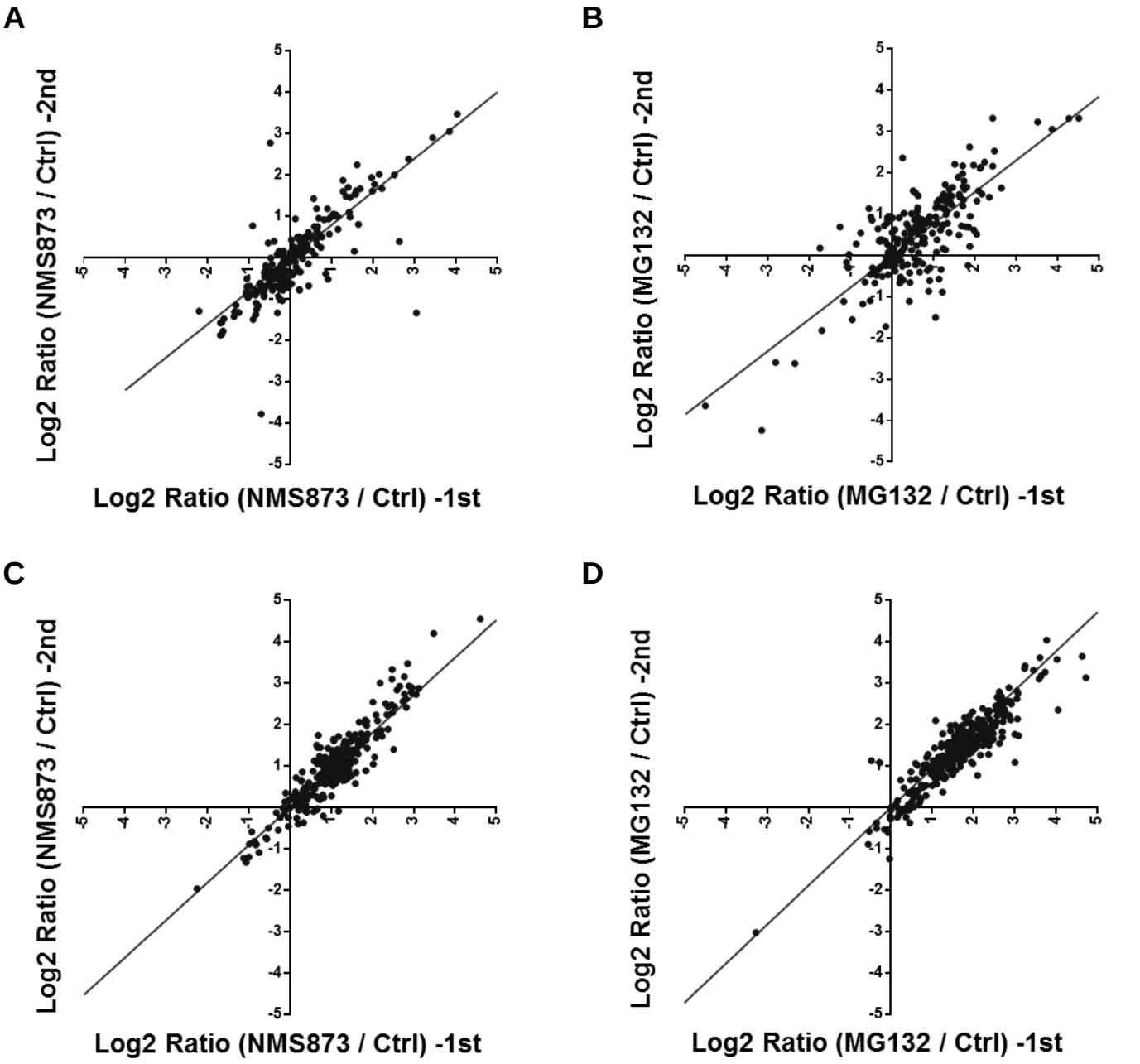

Supplemental Fig. 6

Predicted adaptor substrates by covariance:

(Accompanies Fig. 7B)

NPLOC4:
CHCHD3, FAF2, NEDD8, NOP58, RALY, RCN1, STT3A, TXN, UBAC2, UBXN7, UFD1L, VDAC1
UFD1L:
NPLOC4, UBXN7
UBXN7:
RCN1, TXN, UFD1L
FAF2:
ACTG1, ANXA5, ANXA6, CALM1, CUL2, CUL4B, ERLIN1, ERLIN2, PPP1CA, RNF5, SEL1L, SYVN1, TMUB1, UBAC2
FAF1:
ACSL3, ARL6IP5, ARMCX3, ASPH, ATL3, ATP6AP2, BAG2, BCAP31, BRIX1, BSG, C6orf120, CCT8, COPS3, CPT1A, CUL1, CUL3, CUL4B, CYB5B, DDB1, DDX1, DERL2, DNAJB11, DNAJB12, DNM1L, DYNLL1, ERLEC1, ERLIN1, FADS2, FAM8A1, FKBP8, GANAB, GPX8, HERPUD1, HNRNPAB, IMP3, ITGB1, KIAA1967, KPRP, MAGT1, MARCKS, MBOAT7, MCM3, MCM4, MYH14, NACA, NHP2L1, NOL6, OCIAD1, OS9, P4HB, PIGK, POLR2A, PPIB, PPP1CA, PTRH2, QARS, RBM8A, RBX1, RCN2, RDH11, RNF170, RNF5, RPL18A, RPL22, RPL37A, RPS10, SAMM50, SDCBP, SERPINH1, SF1, SKP1, SLC25A11, SNRPF, SPTLC1, SRPRB, SRSF10, SSR3, TCEB1, THRAP3, TMCO1, TMED7, TMED9, TMEM259, TMUB2, TOM1, TOR1AIP1, TP53, TRA2B, TUBB8, UBAP2L, UBE2G2, UBE2K, UGGT1, WDR26, YIPF5, YWHAG
UBXN1:
ALYREF, ASPSCR1, COMT, DSG1, HNRNPF, HNRNPH3, HNRPDL, ILF3, PLAA, SYNCRIP, UBXN4, UBXN6
NSFL1C:
GANAB, GRN, HLA-A, NACA, PPIB, RBX1, RCC1, RPS29, SEC61B, SUMO1, TMEM66
UBXN6:
DNAJB2, DSG1, FUS, PSMA2, PSMA7, PSMB3, SUMO1, TMEM66, UBXN1, UBXN2A
UBXN4:
GNB2L1, PCBP2, PLAA, PSMA4, PSMA5, PSMA6, PSMA7, PSMB1, PSMB2, PSMC1, PSMC2, PSMC4, PSMC6, PSMD1, PSMD11, PSMD12, PSMD13, PSMD2, PSMD3, PSMD7, PSMD8, RPS18, UBE4A, UBQLN1, UBQLN2, UBXN1
UBXN8:
HNRNPH3, TMEM66
UBXN2B, UBXN10, UBXN2A, UBXN11, ASPSCR1:

Supplemental Fig. 7